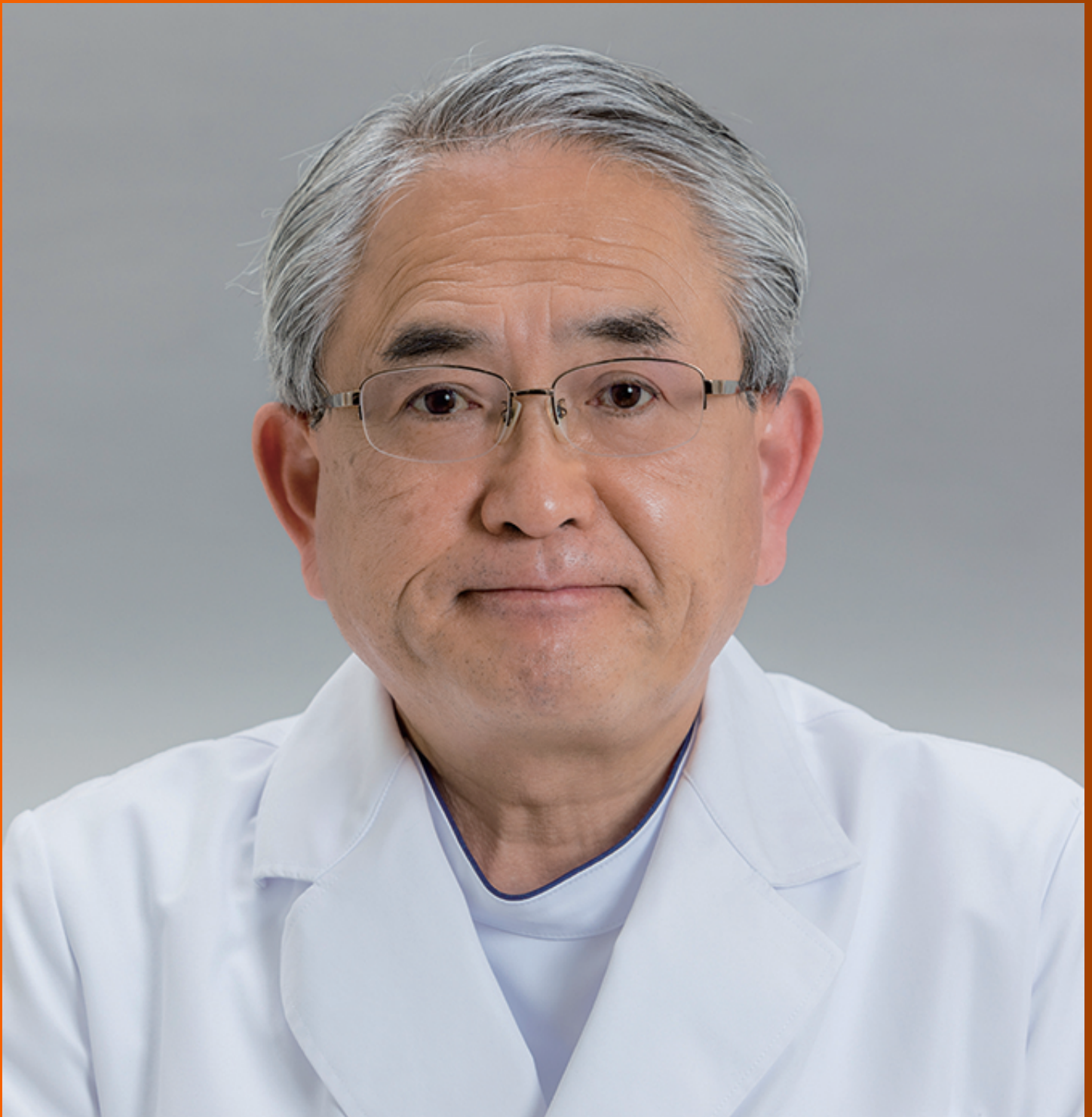


World Journal of *Gastroenterology*

World J Gastroenterol 2024 July 7; 30(25): 3126-3184



EDITORIAL

- 3126 Large non-pedunculated colorectal polyp management: The elephant in the room
Jiang SX, Shahidi N
- 3132 Alanine aminotransferase as a risk marker for new-onset metabolic dysfunction-associated fatty liver disease
Wang D, Zhou BY, Xiang L, Chen XY, Feng JX
- 3140 Refining the targeted population and achieving better for colorectal cancer screening
Zhou NY, Lin YX, Chen LX, Ye LS, Hu B
- 3143 Quantitative assessment of self-management in patients with non-alcoholic fatty liver disease: An unmet clinical need
Borriello R, Esposito G, Mignini I, Gasbarrini A, Zocco MA
- 3147 Risk of hepatic decompensation from hepatitis B virus reactivation in hematological malignancy treatments
Barone M
- 3152 Double-nylon purse-string suture technique: Another addition to the endoscopist's toolbox for full-thickness defect closure
Walia A, Trasolini RP, Shahidi N

ORIGINAL ARTICLE**Retrospective Study**

- 3155 Computed tomography-based radiomics combined with machine learning allows differentiation between primary intestinal lymphoma and Crohn's disease
Xiao MJ, Pan YT, Tan JH, Li HO, Wang HY
- 3166 Predicting hepatocellular carcinoma: A new non-invasive model based on shear wave elastography
Jiang D, Qian Y, Gu YJ, Wang R, Yu H, Dong H, Chen DY, Chen Y, Jiang HZ, Tan BB, Peng M, Li YR

LETTER TO THE EDITOR

- 3179 Scale offers the possibility of identifying adherence to lifestyle interventions in patients with non-alcoholic fatty liver disease
Liu CQ, Hu B
- 3182 Back to the drawing board: Overview of the next generation of combination therapy for inflammatory bowel disease
Lowell JA, Farber MJ, Sultan K

ABOUT COVER

Editorial Board Member of *World Journal of Gastroenterology*, Kentaro Yoshioka, MD, PhD, Director, Center for Liver Diseases, Meijo Hospital, Nagoya 460-0001, Aichi, Japan. kyoshiok8@gmail.com

AIMS AND SCOPE

The primary aim of *World Journal of Gastroenterology* (WJG, *World J Gastroenterol*) is to provide scholars and readers from various fields of gastroenterology and hepatology with a platform to publish high-quality basic and clinical research articles and communicate their research findings online. WJG mainly publishes articles reporting research results and findings obtained in the field of gastroenterology and hepatology and covering a wide range of topics including gastroenterology, hepatology, gastrointestinal endoscopy, gastrointestinal surgery, gastrointestinal oncology, and pediatric gastroenterology.

INDEXING/ABSTRACTING

The WJG is now abstracted and indexed in Science Citation Index Expanded (SCIE), MEDLINE, PubMed, PubMed Central, Scopus, Reference Citation Analysis, China Science and Technology Journal Database, and Superstar Journals Database. The 2024 edition of Journal Citation Reports® cites the 2023 journal impact factor (JIF) for WJG as 4.3; Quartile: Q1. The WJG's CiteScore for 2023 is 7.8.

RESPONSIBLE EDITORS FOR THIS ISSUE

Production Editor: *Hua-Ge Yu*; Production Department Director: *Xu Guo*; Cover Editor: *Jia-Ru Fan*.

NAME OF JOURNAL

World Journal of Gastroenterology

ISSN

ISSN 1007-9327 (print) ISSN 2219-2840 (online)

LAUNCH DATE

October 1, 1995

FREQUENCY

Weekly

EDITORS-IN-CHIEF

Andrzej S Tarnawski

EXECUTIVE ASSOCIATE EDITORS-IN-CHIEF

Xian-Jun Yu (Pancreatic Oncology), Jian-Gao Fan (Chronic Liver Disease), Hou-Bao Liu

EDITORIAL BOARD MEMBERS

<http://www.wjgnet.com/1007-9327/editorialboard.htm>

PUBLICATION DATE

July 7, 2024

COPYRIGHT

© 2024 Baishideng Publishing Group Inc

PUBLISHING PARTNER

Shanghai Pancreatic Cancer Institute and Pancreatic Cancer Institute, Fudan University
Biliary Tract Disease Institute, Fudan University

INSTRUCTIONS TO AUTHORS

<https://www.wjgnet.com/bpg/gcrinfo/204>

GUIDELINES FOR ETHICS DOCUMENTS

<https://www.wjgnet.com/bpg/GerInfo/287>

GUIDELINES FOR NON-NATIVE SPEAKERS OF ENGLISH

<https://www.wjgnet.com/bpg/gcrinfo/240>

PUBLICATION ETHICS

<https://www.wjgnet.com/bpg/GerInfo/288>

PUBLICATION MISCONDUCT

<https://www.wjgnet.com/bpg/gcrinfo/208>

POLICY OF CO-AUTHORS

<https://www.wjgnet.com/bpg/GerInfo/310>

ARTICLE PROCESSING CHARGE

<https://www.wjgnet.com/bpg/gcrinfo/242>

STEPS FOR SUBMITTING MANUSCRIPTS

<https://www.wjgnet.com/bpg/GerInfo/239>

ONLINE SUBMISSION

<https://www.f6publishing.com>

PUBLISHING PARTNER'S OFFICIAL WEBSITE

<https://www.shca.org.cn>
<https://www.zs-hospital.sh.cn>

Retrospective Study

Predicting hepatocellular carcinoma: A new non-invasive model based on shear wave elastography

Dong Jiang, Yi Qian, Yi-Jun Gu, Ru Wang, Hua Yu, Hui Dong, Dong-Yu Chen, Yan Chen, Hao-Zheng Jiang, Bi-Bo Tan, Min Peng, Yi-Ran Li

Specialty type: Gastroenterology and hepatology

Provenance and peer review:

Unsolicited article; Externally peer reviewed.

Peer-review model: Single blind

Peer-review report's classification

Scientific Quality: Grade B

Novelty: Grade B

Creativity or Innovation: Grade A

Scientific Significance: Grade B

P-Reviewer: Reeves HL, United Kingdom

Received: March 7, 2024

Revised: May 22, 2024

Accepted: May 27, 2024

Published online: July 7, 2024

Processing time: 115 Days and 22.7 Hours



Dong Jiang, Yi Qian, Yi-Jun Gu, Ru Wang, Dong-Yu Chen, Yan Chen, Bi-Bo Tan, Yi-Ran Li, Department of Ultrasound, Eastern Hepatobiliary Surgery Hospital, The Third Affiliated Hospital of Naval Medical University, Shanghai 200433, China

Hua Yu, Hui Dong, Department of Pathology, Shanghai Eastern Hepatobiliary Surgery Hospital, Third Affiliated Hospital of Naval Medical University, Shanghai 200433, China

Hao-Zheng Jiang, Department of College of Art and Science, Case Western Reserve University, Cleveland, OH 44106, United States

Min Peng, Ultrasound Diagnosis, PLA Naval Medical Center, Shanghai 200437, China

Co-first authors: Dong Jiang and Yi Qian.

Co-corresponding authors: Min Peng and Yi-Ran Li.

Corresponding author: Yi-Ran Li, MD, Attending Doctor, Department of Ultrasound, Eastern Hepatobiliary Surgery Hospital, The Third Affiliated Hospital of Naval Medical University, No. 225 Changhai Road, Shanghai 200433, China. liyiranehsh@sina.com

Abstract

BACKGROUND

Integrating conventional ultrasound features with 2D shear wave elastography (2D-SWE) can potentially enhance preoperative hepatocellular carcinoma (HCC) predictions.

AIM

To develop a 2D-SWE-based predictive model for preoperative identification of HCC.

METHODS

A retrospective analysis of 884 patients who underwent liver resection and pathology evaluation from February 2021 to August 2023 was conducted at the Oriental Hepatobiliary Surgery Hospital. The patients were divided into the modeling group ($n = 720$) and the control group ($n = 164$). The study included conventional ultrasound, 2D-SWE, and preoperative laboratory tests. Multiple logistic regression was used to identify independent predictive factors for

malignant liver lesions, which were then depicted as nomograms.

RESULTS

In the modeling group analysis, maximal elasticity (Emax) of tumors and their peripheries, platelet count, cirrhosis, and blood flow were independent risk indicators for malignancies. These factors yielded an area under the curve of 0.77 (95% confidence interval: 0.73-0.81) with 84% sensitivity and 61% specificity. The model demonstrated good calibration in both the construction and validation cohorts, as shown by the calibration graph and Hosmer-Lemeshow test ($P = 0.683$ and $P = 0.658$, respectively). Additionally, the mean elasticity (Emean) of the tumor periphery was identified as a risk factor for microvascular invasion (MVI) in malignant liver tumors ($P = 0.003$). Patients receiving antiviral treatment differed significantly in platelet count ($P = 0.002$), Emax of tumors ($P = 0.033$), Emean of tumors ($P = 0.042$), Emax at tumor periphery ($P < 0.001$), and Emean at tumor periphery ($P = 0.003$).

CONCLUSION

2D-SWE's hardness value serves as a valuable marker for enhancing the preoperative diagnosis of malignant liver lesions, correlating significantly with MVI and antiviral treatment efficacy.

Key Words: Shear wave elastography; Predicting model; Microvascular invasion; Antiviral treatment; Hepatocellular carcinoma

©The Author(s) 2024. Published by Baishideng Publishing Group Inc. All rights reserved.

Core Tip: This study pioneers a new model utilizing two-dimensional shear wave elastography (2D-SWE) to enhance preoperative diagnosis of hepatocellular carcinoma. This study highlights the prognostic value of 2D-SWE stiffness values in assessing malignant liver lesions in patients with chronic hepatitis B, their microvascular invasion potential, and monitoring the efficacy of antiviral treatments. The predictive map validated by receiver operating characteristic analysis provides a promising tool for clinicians in the management of liver cancer and represents an important step forward in precision oncology.

Citation: Jiang D, Qian Y, Gu YJ, Wang R, Yu H, Dong H, Chen DY, Chen Y, Jiang HZ, Tan BB, Peng M, Li YR. Predicting hepatocellular carcinoma: A new non-invasive model based on shear wave elastography. *World J Gastroenterol* 2024; 30(25): 3166-3178

URL: <https://www.wjgnet.com/1007-9327/full/v30/i25/3166.htm>

DOI: <https://dx.doi.org/10.3748/wjg.v30.i25.3166>

INTRODUCTION

The global incidence of liver cancer continues to rise, affecting over a million people annually. This trend underscores the urgent need to address liver cancer[1,2]. Hepatocellular carcinoma (HCC) represents approximately 90% of liver cancer cases in China and is strongly associated with hepatitis B virus (HBV) exposure[3,4]. Surgery remains the principal therapeutic strategy for malignant liver tumors, depending on patient condition and liver function evaluation[5]. Kim *et al*[6] investigated the accuracy of preoperative diagnosis through studies utilizing ferumoxides-enhanced and mangafodipir trisodium-enhanced magnetic resonance imaging for diagnosing HCC. Additionally, Liu *et al*[7] explored the viscoelastic properties of proliferative HCC using three-dimensional (3D) magnetic resonance elastography (MRE). The relationship between preoperative carcinoembryonic antigen levels and resectability, prognosis, and survival in patients with colorectal liver metastases has also been examined[8]. Consequently, assessing hardness has become a common practice in pre-hepatectomy evaluations.

Two-dimensional shear wave elastography (2D-SWE) is a validated ultrasound elastography technique with multiple advantages. It provides precise regions of interest (ROI) and monitors blood flow changes for accurate measurements. Emerging evidence supports 2D-SWE for fibrosis staging in patients with chronic HB[9]. Liver stiffness measurements obtained *via* transient elastography are also used to assess the risk of liver cancer following antiviral therapy for chronic hepatitis B (CHB)[10]. The APS score, based on 2D-SWE, predicts liver cancer likelihood within 5 years[11]. Shear wave velocity (SWV) in liver metastasis from colorectal cancer offers prognostic insights for chemotherapy recipients, where a decrease in SWV after the second day of chemotherapy indicates a favorable outcome[12]. Moreover, liver elasticity imaging helps predict postoperative complications[13] and recurrence[14] in HCC patients. Current research using 2D-SWE to differentiate malignant from benign focal liver lesions is ongoing, though it faces limitations in sample size, and a preoperative model for predicting malignant liver tumors has yet to be established[15].

Our contribution involves a pioneering liver malignancy prediction model utilizing 2D-SWE to measure hardness values. This approach culminated in a constructed nomogram, with model validation executed on prospective cases. The prediction model demonstrated an area under the receiver operating characteristic (ROC) curve (AUC) of 0.77, with a 95% confidence interval (CI) ranging from 0.73 to 0.81. Additionally, the model achieved a sensitivity of 84% and a specificity of 61%. The results of the calibration plot and Hosmer-Lemeshow test, with respective P values of 0.683 and

0.658, indicate that there is good calibration observed in both the deduction and validation cohorts. This innovative model marks a significant step towards enhanced liver tumor prediction.

MATERIALS AND METHODS

Structure and patient recruitment

The current study obtained ethical approval from our institution's Ethics Committee (Ethics No: EHBHKY2021-K-011). All patients provided written informed consent before undergoing ultrasound examinations. This single-center, retrospective study introduced a novel non-invasive diagnostic model that merges ultrasound elastography with laboratory analyses to detect malignant liver lesions. Data spanning from February 2021 to February 2023 were utilized to develop a predictive model, while data from March 2023 to August 2023 were employed for validation.

A total of 884 patients were enrolled in the study, divided into the modeling group ($n = 720$) and the validation group ($n = 164$). These patients met specific criteria[16,17]: Conventional ultrasound identified one or more solid liver lesions with a maximum depth of less than 8 cm. In SWE quality mode, liver cancer lesions appeared green, indicating accurate SWE measurements. Exclusion criteria included: Refusal to participate; patients under 18 years; lack of a definitive final diagnosis, with the exception of non-liver malignant metastases requiring post-operative pathological confirmation; and a history of local radiotherapy or chemotherapy treatments such as ablation, proton therapy, and transarterial chemoembolization.

Conventional ultrasound and 2D-SWE evaluation

We utilized the Acuson Sequoia diagnostic ultrasound system (Siemens Healthineers, Mountain View, CA, United States) and a convex abdominal transducer (5C1) for conventional ultrasound examinations. Patients were required to fast for at least 8 hours prior to the procedure. An experienced ultrasound physician with over 15 years of experience performed liver scans to detect solid lesions. The dimensions of each lesion were measured, and lesion volume was calculated using the formula[18]: $V = 0.5 LW^2$ (V: Volume; L: Length; W: Width). The ultrasound physician assessed each lesion as benign, malignant, or undetermined based on features such as number, diameter, shape, margins, echogenicity, and blood flow characteristics of the lesions and surrounding liver tissue. Features of cirrhosis observed included irregular liver shape, uneven capsule contour, heterogeneous echogenicity distribution, portal vein enlargement, spleen enlargement, and abdominal fluid accumulation.

Following conventional ultrasound, a second specialist with expertise in ultrasound elastography conducted 2D-SWE evaluations using the same equipment and probe. No pressure was applied during this evaluation. Upon activating the 2D-SWE mode, the targeted liver cancer lesion was displayed. A ROI was defined, encompassing the lesion and adjacent liver tissue. The lesion appeared green in the image's quality feature (Figure 1A), indicating the 2D-SWE image met the required quality standard. The velocity scale ranged from 0.5 m/s to 4.0 m/s (Figure 1B). Spherical ROIs were placed on the firmest part of the tumor and its periphery. Max values of ROIs were maximal elasticity (E_{max}) (Figure 1C); average was mean elasticity (E_{mean})[19]. Three SWE measurements were obtained for each lesion[20].

Laboratory investigations and histological assessment

Preoperative laboratory investigations included liver function tests, complete blood count, renal function tests, coagulation profiles, hepatitis virus-related tests, and other necessary examinations.

Histological specimens were stained and independently evaluated by two experienced pathologists (with over 10 years of expertise) using the NAS scoring system. For malignancies, it was crucial to assess the presence of tumor thrombi in the small veins adjacent to the tumors (Figure 1D).

Statistical analysis

Statistical analyses were performed using SPSS Statistics 28 (IBM, Chicago, IL, United States) and R programming language version 4.0.3. Continuous variables were reported as means \pm SD. The comparison of continuous variables was performed using either a *t*-test or a Mann-Whitney *U* test. Variables were categorized based on clinical outcomes, and their distributions were presented as counts and percentages. The analysis of these categorical variables employed either Fisher's exact test or the chi-squared test. A logistic regression model included all pertinent factors, and only variables that showed statistical significance ($P < 0.05$) were incorporated into a multivariate logistic regression model using an advanced sequential approach to calculate odds ratios (ORs). Variables with an AUC > 0.7 were considered significant. Nomogram efficiency was assessed using the concordance index (C-index). The model's validity was confirmed in the validation cohort using R software.

RESULTS

Overall, the model was established using independent risk indicators for malignant lesions, achieving an AUC of 0.77 with a 95%CI ranging from 0.73 to 0.81. The study findings showed sensitivity and specificity rates of 84% and 61%, respectively. The calibration graph and Hosmer-Lemeshow test highlighted good calibration in both the construction and validation cohorts ($P = 0.683$ and $P = 0.658$, respectively). Additionally, E_{mean} at the tumor periphery was identified as a risk factor for microvascular invasion (MVI) in malignant liver tumors ($P = 0.003$). A comprehensive comparison between

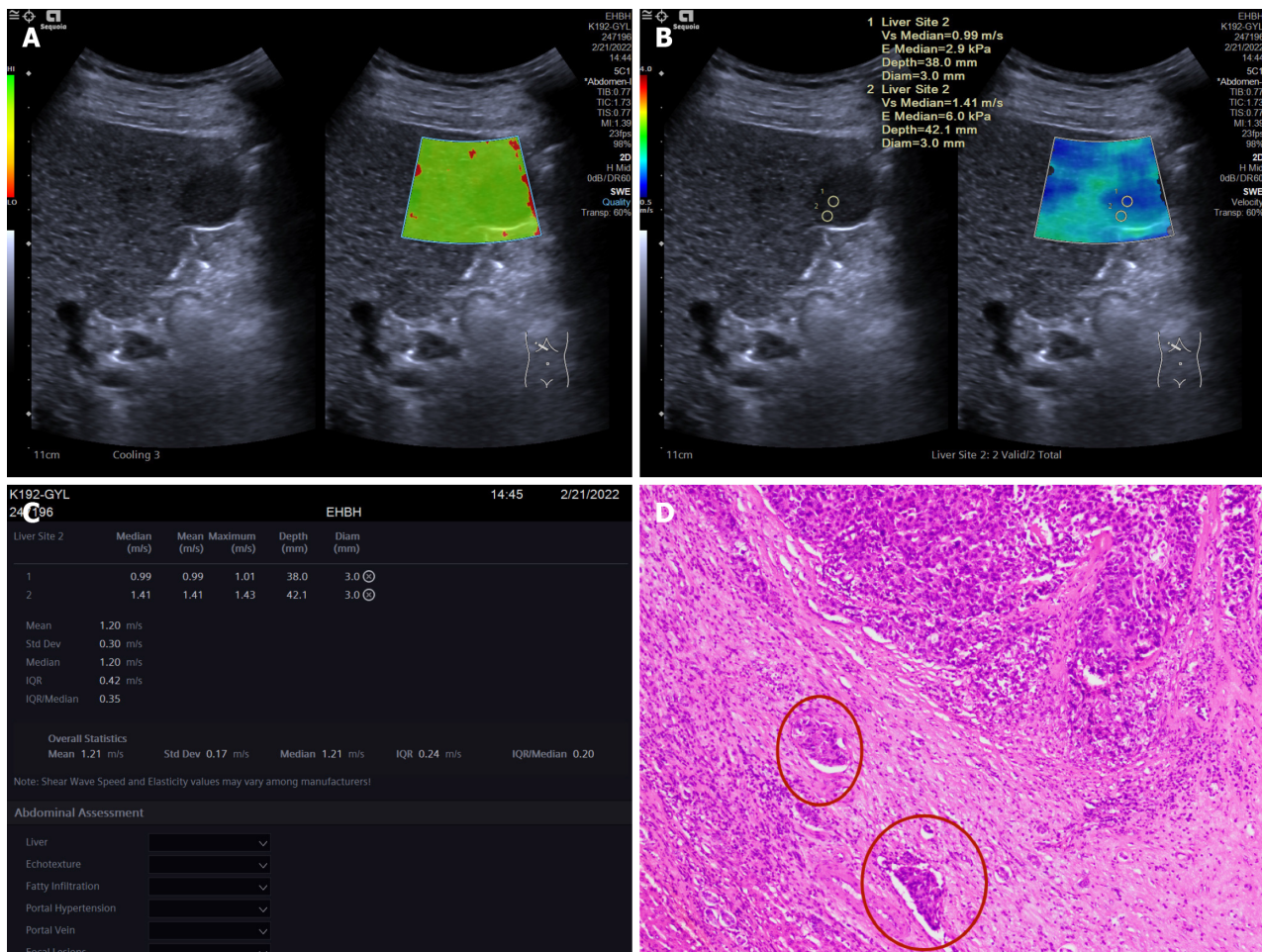


Figure 1 2D shear wave elastography was used to assess localized liver lesions in this study. A: Demonstrates tumors displayed in the green mass mode, indicating that 2D shear wave elastography’s accuracy meets the standard. For tumors displayed in speed mode, its velocity scale was configured within the range of 0.5 to 4.0 m/s; B: Shows two round areas of interest (ROIs) placed at the hardest part of the tumor and around the tumor, each with a diameter of 3 mm; C: The maximum elasticity of these ROIs, denoted as maximal elasticity, was recorded; D: Illustrates intracapsular vascular tumor emboli, highlighted in the image (HE × 100).

patients who received antiviral treatment and those who did not showed statistically significant differences in platelet count ($P = 0.002$), Emax of tumors ($P = 0.033$), Emean of tumors ($P = 0.042$), Emax at the tumor periphery ($P < 0.001$), and Emean at the tumor periphery ($P = 0.003$).

Baseline patient characteristics

A total of 800 patients underwent simultaneous ultrasound examinations, laboratory tests, and liver biopsies in the experimental cohort, with an average age of 55.2 years ± 12.0 years (Table 1). However, 80 patients were excluded for various reasons: Under 18 years of age ($n = 12$), refusal to participate ($n = 7$), failed or inconclusive biopsies ($n = 5$), or history of local radiotherapy or chemotherapy ($n = 56$) (Figure 2). The validation cohort included 200 patients who underwent the same procedures, with an average age of 55.1 years ± 10.4 years (Supplementary Table 1). Among them, 36 patients were excluded as they were under 18 years of age ($n = 4$), refusal to participate ($n = 5$), failed/inconclusive biopsies ($n = 3$), or a history of local radiotherapy or chemotherapy ($n = 24$) (Figure 2).

Within the experimental cohort, 520 patients had liver malignancies: 413 with HCC, 55 with intrahepatic cholangiocarcinoma, and 52 with liver metastases. The average age was 55.5 years ± 11.8 years. Notably, 101 of these patients exhibited signs of MVI, while 419 did not (Supplementary Table 2).

Among the experimental cohort, 307 patients had CHB, with an average age of 55.1 years ± 11.1 years. Of these, 159 received antiviral treatment (entecavir or tenofovir as first-line treatment), while 148 did not receive treatment (Supplementary Table 3).

Liver cancer-associated factors and predictive values

In the experimental cohort, univariable analysis identified correlations between liver cancer and several factors, including platelet count, cirrhosis, blood flow, Emax of tumors, Emean of tumors, Emax at the tumor periphery, and Emean at the tumor periphery (Table 2). Multivariable analysis revealed that five factors were significantly associated with the occurrence of liver cancer: Platelet count ($P < 0.001$; OR: 1.00, 95%CI: 0.99-1.00), cirrhosis ($P = 0.027$; OR: 0.61, 95%CI: 0.40-0.95), blood flow ($P < 0.001$; OR: 2.51, 95%CI: 1.72-3.67), Emax of tumors ($P < 0.001$; OR: 2.08, 95%CI: 1.50-2.89), and

Table 1 The initial patient features of the experimental cohort were assessed, *n* (%)

Variable	All patients (n = 720)	Benign (n = 200)	Malignant (n = 520)	P value [†]
Clinical data				
Age (years)	55.2 ± 12.0	54.6 ± 12.5	55.5 ± 11.8	0.353
Sex (%)				0.423
Men	572 (79.4)	155 (77.5)	417 (80.2)	
Women	148 (20.6)	45 (22.5)	103 (19.8)	
Body mass index (kg/m ²)	24.0 ± 3.3	23.9 ± 3.2	24.0 ± 3.4	0.678
Nationality (%)				0.361
Han nationality	698 (96.9)	192 (96)	506 (97.3)	
Not Han nationality	22 (3.1)	8 (4)	14 (2.7)	
History of tumor (%)				0.210
Yes	62 (8.6)	13 (6.5)	49 (9.4)	
No	658 (91.4)	187 (93.5)	471 (90.6)	
Laboratory data				
ALT (IU/L)	44.6 ± 105.4	37.8 ± 60.3	47.2 ± 118.2	0.284
AST (IU/L)	41.5 ± 100.5	34.8 ± 62.1	44 ± 111.8	0.269
GGT (IU/L)	83.9 ± 126.4	75.1 ± 139.3	87.4 ± 121.0	0.243
Prothrombin time (s)	12.1 ± 3.1	11.9 ± 1.2	12.2 ± 3.6	0.356
INR	1.0 ± 0.4	1.0 ± 0.1	1.0 ± 0.5	0.372
PLT (10 ⁹ /L)	182.1 ± 73.2	207.4 ± 73.7	172.4 ± 70.7	< 0.001
Albumin (g/L)	41.3 ± 4.1	41.3 ± 4.9	41.4 ± 3.8	0.780
Total bilirubin (μmol/L)	67.6 ± 5.3	67.5 ± 5.5	67.7 ± 5.3	0.638
Ultrasonic data				
Single	562 (78.1)	143 (71.5)	419 (80.6)	
Multiple	158 (21.9)	57 (28.5)	101 (19.4)	
Diameter (cm)	5.3 ± 3.0	5.2 ± 3.5	5.3 ± 2.8	0.629
Shape (%)				0.102
Roundness	363 (50.4)	91 (45.5)	272 (52.3)	
Ellipse	357 (49.6)	109 (54.5)	248 (47.7)	
Echo (%)				0.064
Hypoecho	236 (32.8)	76 (38.0)	160 (30.8)	
Hyperecho	484 (67.2)	124 (62.0)	360 (69.2)	
Edge (%)				0.010
Smooth	398 (55.3)	126 (74.4)	272 (52.3)	
Coarse	322 (44.7)	74 (25.6)	248 (47.7)	
Cirrhosis (%)				< 0.001
Yes	239 (33.2)	35 (17.5)	204 (39.2)	
No	481 (66.8)	165 (82.5)	316 (60.8)	
Blood (%)				< 0.001
Yes	462 (64.2)	97 (48.5)	365 (70.2)	
No	258 (35.8)	103 (51.5)	155 (29.8)	
Emax of the tumors (m/s)	2.4 ± 1.0	2.1 ± 0.6	2.5 ± 1.1	< 0.001

Emean of the tumors (m/s)	1.8 ± 0.5	1.6 ± 0.4	1.9 ± 0.5	< 0.001
Emax of the periphery of tumors (m/s)	1.6 ± 1.0	1.3 ± 0.4	1.7 ± 1.2	< 0.001
Emean of the periphery of tumors (m/s)	1.5 ± 0.7	1.3 ± 0.4	1.5 ± 0.7	< 0.001

¹P value for comparisons between benign cohort and malignant cohort.

The data enclosed between parenthesis represents the intervals of confidence at 95%. ALT: Alanine aminotransferase; AST: Aspartate aminotransferase; GGT: G-glutamyl transferase; PLT: Platelet count; Emax: Maximal elasticity; Emean: Mean elasticity.

Table 2 Both univariable and multivariable logistic regression approaches to assess the probability of liver cancer in the experimental cohort (n = 720)

Variable	Univariable		Multivariable	
	Odds ratio	P value	Odds ratio	P value
Clinical data				
Age (years)	1.00 (0.99, 1.02)	0.352		
Sex (%)	0.85 (0.57, 1.26)	0.424		
Body mass index (kg/m ²)	1.01 (0.96, 1.06)	0.678		
Nationality (%)	0.66 (0.27, 1.61)	0.364		
History of tumor (%)	1.50 (0.79, 2.82)	0.213		
Laboratory data				
ALT (IU/L)	1.00 (0.99, 1.00)	0.306		
AST (IU/L)	1.00 (0.99, 1.00)	0.299		
GGT (IU/L)	1.00 (0.99, 1.00)	0.249		
Prothrombin time (s)	1.00 (0.93, 1.24)	0.328		
INR	2.94 (0.50, 17.38)	0.235		
PLT (10 ⁹ /L)	1.00 (0.99, 1.00)	< 0.001	1.00 (0.99, 1.00)	< 0.001
Albumin (g/L)	1.00 (0.97, 1.05)	0.780		
Total bilirubin (μmol/L)	1.01 (0.98, 1.04)	0.638		
Ultrasonic data				
Number (%)	0.61 (0.42, 0.89)	0.009	0.61 (0.40, 0.95)	0.027
Diameter (cm)	1.01 (0.96, 1.07)	0.628		
Shape (%)	0.76 (0.55, 1.06)	0.102		
Echo (%)	1.38 (0.98, 1.94)	0.065		
Edge (%)	1.56 (1.11, 2.17)	0.010		
Cirrhosis (%)	3.04 (2.03, 4.57)	< 0.001		
Blood (%)	2.50 (1.79, 3.50)	< 0.001	2.51 (1.72, 3.67)	< 0.001
Emax of the tumors (m/s)	2.86 (2.10, 3.91)	< 0.001	2.08 (1.50, 2.89)	< 0.001
Emean of the tumors (m/s)	3.95 (2.60, 6.01)	< 0.001		
Emax of the periphery of tumors (m/s)	5.72 (3.51, 9.34)	< 0.001		
Emean of the periphery of tumors (m/s)	5.84 (3.54, 9.63)	< 0.001	2.70 (1.54, 4.73)	0.001

The data enclosed between parenthesis represents the intervals of confidence at 95%. ALT: Alanine aminotransferase; AST: Aspartate aminotransferase; GGT: G-glutamyl transferase; PLT: Platelet count; Emax: Maximal elasticity; Emean: Mean elasticity.

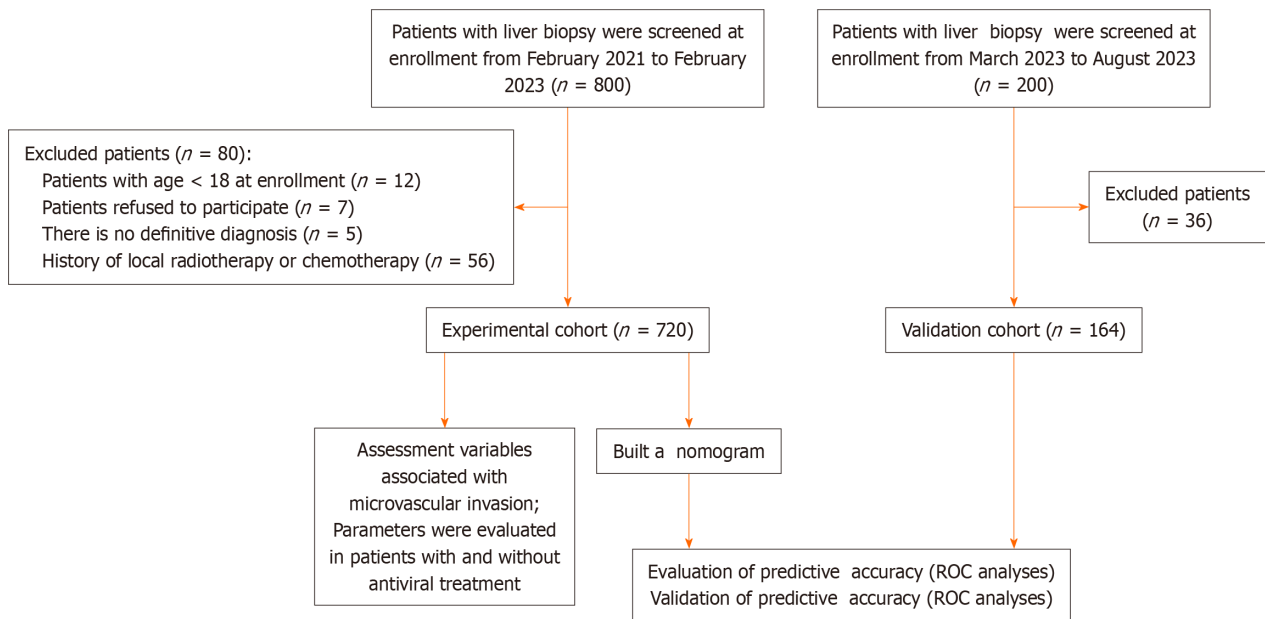


Figure 2 The flowchart depicted herein presents the patient enrollment process in the study. ROC: Receiver operating characteristic.

E_{mean} at the tumor periphery ($P = 0.001$; OR: 2.70, 95%CI: 1.54-4.73). **Figure 3** graphically represents the results of the multivariable analysis for predicting liver cancer. The risk score was calculated using the following formula: Risk score = (cirrhosis \times 0.610) + (blood flow \times 0.920) + (E_{max} of tumors \times 0.733) + (E_{mean} at the tumor periphery \times 0.993) - (platelets \times 0.005) - (cirrhosis \times 0.487).

Univariable logistic regression analysis based on these five parameters demonstrated excellent discriminatory performance in detecting liver cancer. Performance metrics were as follows: The AUC was 0.77 (95%CI: 0.73, 0.81). Sensitivity was 84%, specificity was 61%, positive predictive value was 85%, negative predictive value was 60%, and overall diagnostic accuracy was 78% (Table 3).

The development of a predictive nomogram for liver cancer

A meticulously designed nomogram incorporating the five previously identified predictors was developed (Figure 4A). The model's excellent calibration in both the development and validation cohorts is demonstrated by the calibration curve and the Hosmer-Lemeshow test results ($P = 0.683$ and $P = 0.658$, respectively) (Figure 4B and C). Notably, the derivation cohort displayed a C-index of 0.767, while the verification cohort reached 0.743, confirming the model's strong discriminatory capacity.

Factors associated with MVI state

Exploring the MVI state, the single-factor analysis within the liver cancer patients of the predictive model revealed a significant correlation between E_{mean} of tumors ($P = 0.001$; OR: 2.70, 95%CI: 1.54-4.73) and the presence of MVI (Supplementary Table 4).

Comparison analysis in chronic hepatitis B patients: Treated vs untreated

Analysis of 307 CHB patients in the experimental cohort, including 159 who received oral antiviral treatment and 148 untreated, showed significant differences between the groups in several indicators: Platelets ($P = 0.002$), E_{max} of tumors ($P = 0.033$), E_{mean} of tumors ($P = 0.042$), E_{max} at the tumor periphery ($P < 0.001$), and E_{mean} at the tumor periphery ($P = 0.003$) (Supplementary Table 3). Notably, treated patients exhibited reduced tissue stiffness in both tumors and adjacent tissue, as indicated by lower elasticity values (Figure 5).

DISCUSSION

In this study, we developed a liver cancer prediction model by integrating conventional ultrasound and 2D-SWE techniques with laboratory tests. The ROC curve constructed for the model yielded an AUC of 0.77, demonstrating significant diagnostic utility. This predictive model is promising for the preoperative evaluation of liver lesions and the formulation of treatment strategies. 2D-SWE, a widely used liver elastography technique, plays a crucial role in the identification and assessment of hepatic illnesses and the evaluation of fibrotic conditions affecting the liver[21,22]. Despite ongoing debates regarding the differential diagnosis of liver lesions using 2D-SWE, consensus has yet to be reached[23,24]. We utilized E_{max} and E_{mean} as quantitative parameters to measure the hardness of liver lesions[25]. The findings showed robust predictive value in the model group, where E_{max} of tumors (AUC = 0.67) and E_{mean} at the

Table 3 Diagnostic performance of multivariable model, maximal elasticity of the tumors, mean elasticity of the periphery of tumors, platelet count, cirrhosis, blood and number for the diagnosis of malignant tumor in the experimental cohort (*n* = 720)

Parameter	AUC	Cutoff value ¹	Sensitivity (%)	Specificity (%)	Positive predictive value (%)	Negative predictive value (%)	Diagnostic accuracy (%)
Multivariable model	0.77 (0.73, 0.81)	0.653	84	61	85	60	78
Emean of the periphery of tumors	0.69 (0.64, 0.73)	1.375	59	71	84	40	62
Emax of the tumors	0.67 (0.63, 0.72)	2.205	61	65	82	39	62
Edge echo	0.61 (0.57, 0.65)	0.500	39	83	85	34	51
Blood	0.62 (0.56, 0.66)	0.500	70	52	79	40	65
Number	0.46 (0.41, 0.50)	0.500	19	72	64	25	34
PLT	0.34 (0.30, 0.39)	39.500	100	1	72	5	72

¹Cutoff values that maximized the sum of sensitivity and specificity were chosen.

PLT: Platelet count; Emax: Maximal elasticity; Emean: Mean elasticity; AUC: Area under the curve.

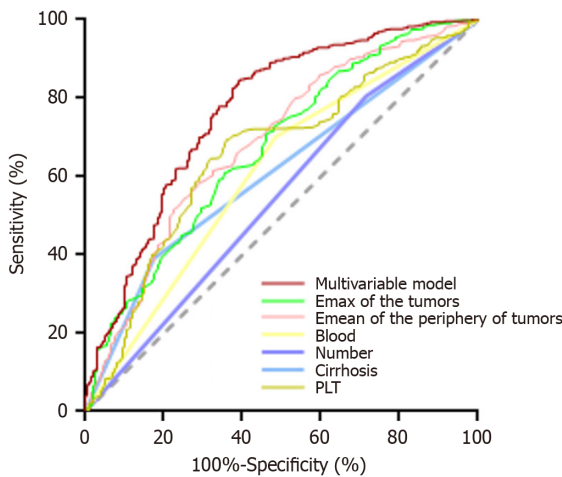


Figure 3 The graphs in this figure display receiver operating characteristic curves, which indicate the accuracy of different predictive parameters in predicting hepatic malignant tumors in the experimental cohort. PLT: Platelet count.

tumor periphery (AUC = 0.69) emerged as strong indicators. This outcome could be attributed to our measurements, which captured not only the intrinsic hardness of the lesions but also assessed the hardness of the surrounding areas. It is noteworthy that ischemic necrosis often occurs in the central region of tumors, affecting their hardness. Additionally, reports suggest that the tissue surrounding the tumor might exhibit greater hardness compared to the central region[26].

The established model identified cirrhosis, blood flow, platelet count, and tumor number as risk factors for predicting malignant tumors. This research significantly contributes by elucidating the incidence and levels of HBV DNA in non-symptomatic HBV carriers, patients with cirrhosis, and cases of HCC originating from The Gambia. It also aimed to evaluate the potential risk of developing cirrhosis or HCC in relation to HBV viremia[27]. In another study, Pereira *et al* [28] hypothesized that activation of the Hedgehog pathway is observed during the fibrogenic healing process of liver damage caused by chronic viral hepatitis. They suggested that cells responsive to Hedgehog signaling might contribute to disease progression and hepatocarcinogenesis in individuals with chronic viral hepatitis. Beste *et al*[29] aimed to quantify the burden of cirrhosis and HCC by their underlying causes from 2001 to 2013. Kanwal *et al*[30] assessed the risk of developing HCC in individuals with non-alcoholic fatty liver disease (NAFLD). Malignant tumors are often characterized by abundant blood supply and a propensity for metastatic lesions, which is why routine ultrasound frequently detects multiple blood flows. In their study, Chon *et al*[31] conducted a comparative analysis to evaluate the accuracy of non-invasive liver fibrosis prognosis techniques in predicting the occurrence of HCC among individuals diagnosed with CHB.

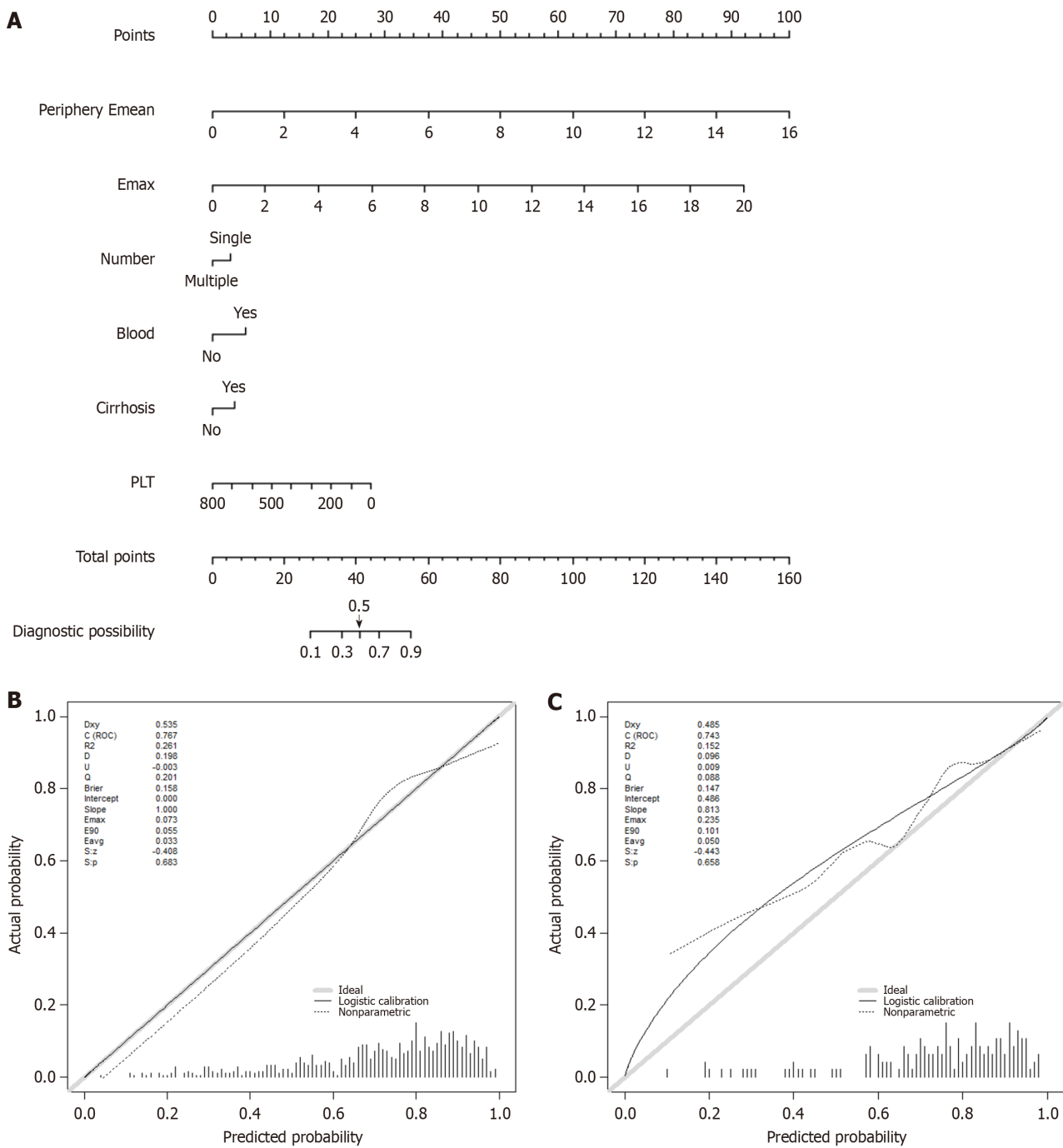


Figure 4 This figure demonstrates the process of generating and evaluating the nomogram. A: Presents the nomogram used for predicting malignant tumors; B and C: Depict the calibration curve, providing estimates of malignant tumors using the nomogram in the development and confirmation cohorts, respectively.

The aspartate platelet count ratio index (APRI) is widely recognized as an indicator for assessing liver fibrosis and cirrhosis[32], primarily used to predict the survival rate of HCC patients post-hepatectomy. By integrating inflammation-based predictive scores, the combination of APRI and these scores enhances the accuracy of prognostic predictions. Kim *et al*[33] suggest using modified PAGE-B scores to improve predictive performance.

MVI is characterized by the presence of cancer cell clusters within blood vessels, surrounded by endothelial cells, as observed under a microscope. Commonly found within the tumor stroma, tumor capsule, and peritumoral region, MVI frequently occurs in branches of the portal vein adjacent to non-cancerous liver tissue. As the disease progresses, the incidence of MVI increases, establishing it as a predictive marker for tumor prognosis. This study assessed the impact of MVI in small HCCs up to 2 cm. In patients with small HCCs, MVI did not affect long-term survival ($P = 0.8$); however, in those with larger HCCs, the presence of MVI significantly reduced survival outcomes ($P < 0.0001$)[34]. Multivariate logistic regression analysis identified independent predictors of MVI: The radioactive materials score, alpha-fetoprotein levels, and tumor size[35]. Radiomics offers potential in predicting MVI[36,37]. In this research, we identified the mean echogenicity of the tumor as a unique independent risk factor for MVI, a significant discovery with implications for

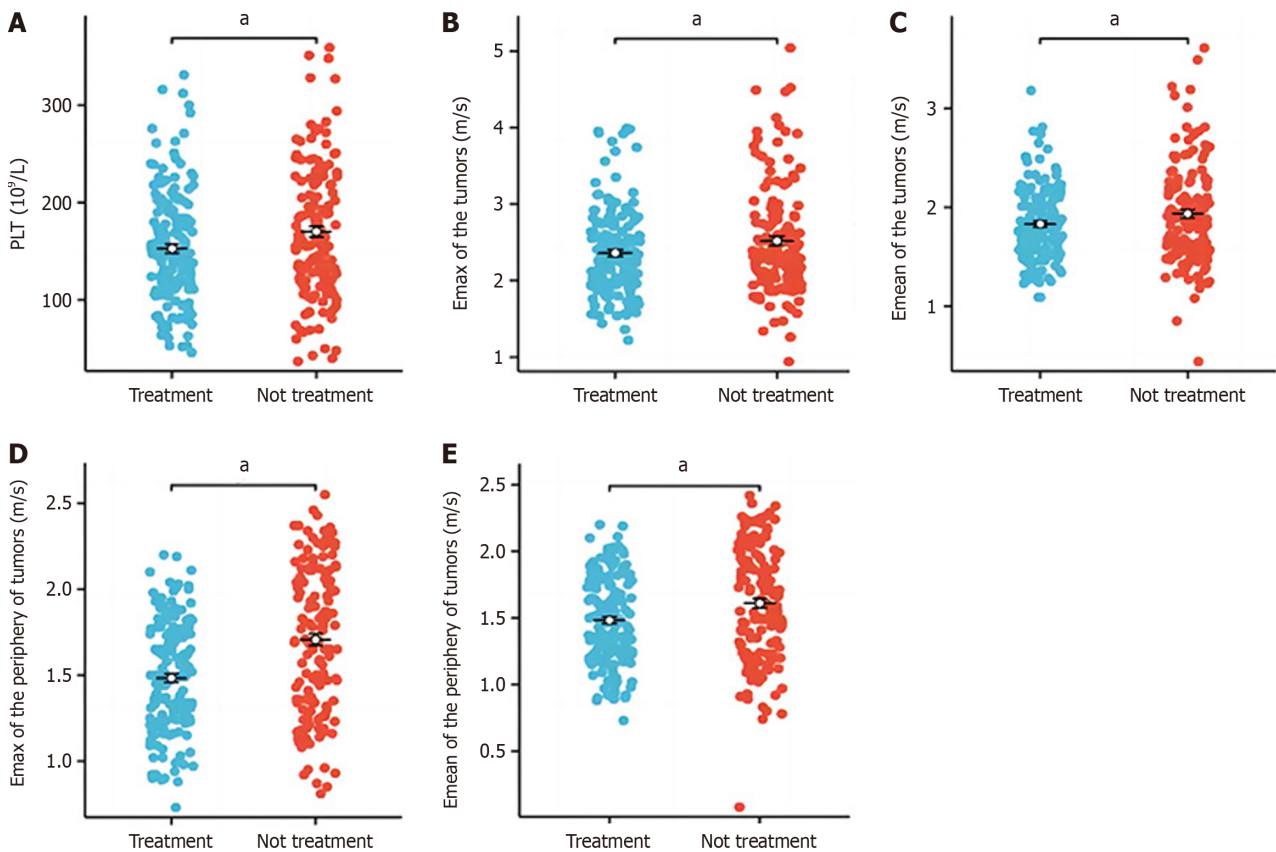


Figure 5 Plots show the distribution of maximal elasticity and mean elasticity within tumors, as well as the maximal elasticity and mean elasticity in the peripheral regions of tumors, along with the mean elasticity count in patients with and without antiviral treatment. PLT: Platelet count; Emax: Maximal elasticity; Emean: Mean elasticity. ^a $P < 0.05$, ^b $0.05 < P < 0.001$, ^c $P < 0.001$.

preoperative MVI assessment.

Previous studies have shown a higher likelihood of liver cancer in patients with cirrhosis. A risk model for antiviral treatment in early-stage CHB infection, using entecavir or tenofovir, integrates age, platelet count, progression of cirrhosis, and cirrhosis value to establish a novel scoring chart (scores 0-304).

These factors are independently associated with an increased risk of HCC, positivity for hepatitis B e-antigen, and levels of serum albumin and total bilirubin[38]. Additionally, research has shown the effectiveness of combining 2D-SWE and MRE in stratifying the probability of HCC occurrence in patients who have achieved hepatitis C virus eradication. This combination is highly effective in identifying patients at high risk for HCC development. Ultrasound elastography precedes MRE if 2D-SWE yields high values, assessing liver stiffness[39]. Our hypothesis suggests that liver stiffness is not only indicative of HCC risk but also correlates with the effectiveness of antiviral treatment. Consequently, the highest and mean elasticity measurements were selected as indicators of liver hardness in 2D-SWE. After antiviral treatment, liver stiffness noticeably decreased.

With the advancement of comprehensive treatment approaches for liver cancer, the importance of preoperative assessment of liver lesions in shaping treatment and prognosis has become increasingly recognized. By employing ultrasound and laboratory tests, we have established a novel, non-invasive method for predicting malignant liver lesions that boasts high sensitivity and specificity, and shows promise for broader application. Specifically, the indicators Emax and Emean, derived from 2D-SWE within the model, demonstrate strong predictive value in assessing liver stiffness. Moreover, in our cohort, Emean of the tumor has been identified as an independent risk factor for MVI in liver cancer, thus confirming a correlation between stiffness and malignancy.

This finding aligns with results from previous studies on the varying hardness of different malignant liver lesions[15]. In the context of antiviral treatment for CHB, the hardness indicators associated with 2D-SWE also show differences in treatment outcomes, highlighting stiffness as a marker of treatment efficacy for liver cancer.

CONCLUSION

In conclusion, integrating hardness indicators from 2D-SWE with laboratory tests forms a robust, non-invasive predictive model for liver cancer, offering significant predictive value for assessing risk and evaluating treatment efficacy. The clinical utility of 2D-SWE-derived hardness indicators goes beyond risk assessment and supports widespread adoption.

FOOTNOTES

Author contributions: Li YR, Jiang D, Qian Y, Wang R, Chen DY, and Tan BB designed the research study; Jiang HZ, Gu YJ, Yu H, Peng M, and Dong H performed the research; Chen Y, Qian Y, Wang R, and Jiang HZ contributed new reagents and analytic tools; Jiang D, Li YR, Tan BB, Gu YJ, Peng M, and Yu H analyzed the data and wrote the manuscript; and all authors have read and approved the final manuscript. Jiang D and Qian Y contributed equally to this work as co-first authors; Peng M and Li YR contributed equally to this work as co-corresponding authors. The reasons for designating Peng M and Li YR as co-corresponding authors are that they share the responsibility of guidance, communication, and organization.

Supported by the National Natural Science Foundation of China Youth Training Project, No. 2021GZR003; and Medical-engineering Interdisciplinary Research Youth Training Project, No. 2022YGJC001.

Institutional review board statement: The study was reviewed and approved by the Shanghai Eastern Hepatobiliary Surgery Hospital (Approval No. EHBHKY2023-K034-P001).

Informed consent statement: All study participants, or their legal guardian, provided informed written consent prior to study enrollment.

Conflict-of-interest statement: All the authors have no conflict of interest related to the manuscript.

Data sharing statement: The datasets used and/or analyzed during the current study are available from the corresponding author on reasonable request.

Open-Access: This article is an open-access article that was selected by an in-house editor and fully peer-reviewed by external reviewers. It is distributed in accordance with the Creative Commons Attribution NonCommercial (CC BY-NC 4.0) license, which permits others to distribute, remix, adapt, build upon this work non-commercially, and license their derivative works on different terms, provided the original work is properly cited and the use is non-commercial. See: <https://creativecommons.org/licenses/by-nc/4.0/>

Country of origin: China

ORCID number: Yi-Ran Li 0000-0002-0768-3495.

S-Editor: Chen YL

L-Editor: Webster JR

P-Editor: Zheng XM

REFERENCES

- 1 **Bosch FX**, Ribes J, Díaz M, Cléries R. Primary liver cancer: worldwide incidence and trends. *Gastroenterology* 2004; **127**: S5-S16 [PMID: 15508102 DOI: 10.1053/j.gastro.2004.09.011]
- 2 **Liu YY**, Rajkumar K, Murphy LJ. Hepatic regeneration in insulin-like growth factor binding protein-1 transgenic mice. *J Hepatol* 1999; **30**: 674-680 [PMID: 10207810 DOI: 10.1016/S0168-8278(99)80199-8]
- 3 **Wang FS**, Fan JG, Zhang Z, Gao B, Wang HY. The global burden of liver disease: the major impact of China. *Hepatology* 2014; **60**: 2099-2108 [PMID: 25164003 DOI: 10.1002/hep.27406]
- 4 **Chen JG**, Zhang SW. Liver cancer epidemic in China: past, present and future. *Semin Cancer Biol* 2011; **21**: 59-69 [PMID: 21144900 DOI: 10.1016/j.semcancer.2010.11.002]
- 5 **Liu CY**, Chen KF, Chen PJ. Treatment of Liver Cancer. *Cold Spring Harb Perspect Med* 2015; **5**: a021535 [PMID: 26187874 DOI: 10.1101/cshperspect.a021535]
- 6 **Kim SK**, Kim SH, Lee WJ, Kim H, Seo JW, Choi D, Lim HK, Lee SJ, Lim JH. Preoperative detection of hepatocellular carcinoma: ferumoxides-enhanced *versus* mangafodipir trisodium-enhanced MR imaging. *AJR Am J Roentgenol* 2002; **179**: 741-750 [PMID: 12185056 DOI: 10.2214/ajr.179.3.1790741]
- 7 **Liu G**, Ma D, Wang H, Zhou J, Shen Z, Yang Y, Chen Y, Sack I, Guo J, Li R, Yan F. Three-dimensional multifrequency magnetic resonance elastography improves preoperative assessment of proliferative hepatocellular carcinoma. *Insights Imaging* 2023; **14**: 89 [PMID: 37198348 DOI: 10.1186/s13244-023-01427-4]
- 8 **Bakalakov EA**, Burak WE Jr, Young DC, Martin EW Jr. Is carcino-embryonic antigen useful in the follow-up management of patients with colorectal liver metastases? *Am J Surg* 1999; **177**: 2-6 [PMID: 10037299 DOI: 10.1016/S0002-9610(98)00303-1]
- 9 **Chen S**, Jiang T. Preoperative noninvasive assessment for liver fibrosis in hepatocellular carcinoma patients with chronic hepatitis B: Comparison of two-dimensional shear-wave elastography with serum liver fibrosis models. *Eur J Radiol* 2020; **133**: 109386 [PMID: 33160197 DOI: 10.1016/j.ejrad.2020.109386]
- 10 **Knop V**, Mauss S, Goeser T, Geier A, Zimmermann T, Herzer K, Postel N, Friedrich-Rust M, Hofmann WP; German Hepatitis C-Registry. Dynamics of liver stiffness by transient elastography in patients with chronic hepatitis C virus infection receiving direct-acting antiviral therapy-Results from the German Hepatitis C-Registry. *J Viral Hepat* 2020; **27**: 690-698 [PMID: 32096310 DOI: 10.1111/jvh.13280]
- 11 **Zhang T**, Zhang G, Deng X, Zeng J, Jin J, Zeping H, Wu M, Zheng R. APS (Age, Platelets, 2D Shear-Wave Elastography) Score Predicts Hepatocellular Carcinoma in Chronic Hepatitis B. *Radiology* 2021; **301**: 350-359 [PMID: 34427463 DOI: 10.1148/radiol.2021204700]
- 12 **Lee DH**, Lee JY, Joo I, Kim TY, Han SW, Lee KH. Shear-wave velocity for colorectal cancer liver metastases as a potential prognostic factor after chemotherapy: a preliminary study. *Clin Radiol* 2021; **76**: 224-232 [PMID: 33402260 DOI: 10.1016/j.crad.2020.09.027]

- 13 **Serenari M**, Han KH, Ravaoli F, Kim SU, Cucchetti A, Han DH, Odaldi F, Ravaoli M, Festi D, Pinna AD, Cescon M. A nomogram based on liver stiffness predicts postoperative complications in patients with hepatocellular carcinoma. *J Hepatol* 2020; **73**: 855-862 [PMID: 32360997 DOI: 10.1016/j.jhep.2020.04.032]
- 14 **Zhao Y**, Wu L, Qin H, Li Q, Shen C, He Y, Yang H. Preoperative combi-elastography for the prediction of early recurrence after curative resection of hepatocellular carcinoma. *Clin Imaging* 2021; **79**: 173-178 [PMID: 34087717 DOI: 10.1016/j.clinimag.2021.05.020]
- 15 **Wang W**, Zhang JC, Tian WS, Chen LD, Zheng Q, Hu HT, Wu SS, Guo Y, Xie XY, Lu MD, Kuang M, Liu LZ, Ruan SM. Shear wave elastography-based ultrasonics: differentiating malignant from benign focal liver lesions. *Abdom Radiol (NY)* 2021; **46**: 237-248 [PMID: 32564210 DOI: 10.1007/s00261-020-02614-3]
- 16 **Bo XW**, Li XL, Xu HX, Guo le H, Li DD, Liu BJ, Wang D, He YP, Xu XH. 2D shear-wave ultrasound elastography (SWE) evaluation of ablation zone following radiofrequency ablation of liver lesions: is it more accurate? *Br J Radiol* 2016; **89**: 20150852 [PMID: 26933911 DOI: 10.1259/bjr.20150852]
- 17 **Dietrich CF**, Bamber J, Berzigotti A, Bota S, Cantisani V, Castera L, Cosgrove D, Ferraioli G, Friedrich-Rust M, Gilja OH, Goertz RS, Karlas T, de Knecht R, de Ledinghen V, Piscaglia F, Procopet B, Saftoiu A, Sidhu PS, Sporea I, Thiele M. EFSUMB Guidelines and Recommendations on the Clinical Use of Liver Ultrasound Elastography, Update 2017 (Long Version). *Ultraschall Med* 2017; **38**: e16-e47 [PMID: 28407655 DOI: 10.1055/s-0043-103952]
- 18 **Tomayko MM**, Reynolds CP. Determination of subcutaneous tumor size in athymic (nude) mice. *Cancer Chemother Pharmacol* 1989; **24**: 148-154 [PMID: 2544306 DOI: 10.1007/BF00300234]
- 19 **Tian WS**, Lin MX, Zhou LY, Pan FS, Huang GL, Wang W, Lu MD, Xie XY. Maximum Value Measured by 2-D Shear Wave Elastography Helps in Differentiating Malignancy from Benign Focal Liver Lesions. *Ultrasound Med Biol* 2016; **42**: 2156-2166 [PMID: 27283039 DOI: 10.1016/j.ultrasmedbio.2016.05.002]
- 20 **Park HS**, Kim YJ, Yu MH, Jung SI, Jeon HJ. Shear Wave Elastography of Focal Liver Lesion: Intraobserver Reproducibility and Elasticity Characterization. *Ultrasound Q* 2015; **31**: 262-271 [PMID: 26086459 DOI: 10.1097/RUQ.0000000000000175]
- 21 **Cassinotto C**, Boursier J, de Ledinghen V, Lebigot J, Lapuyade B, Cales P, Hiriart JB, Michalak S, Bail BL, Cartier V, Mouries A, Oberti F, Fouchard-Hubert I, Vergniol J, Aubé C. Liver stiffness in nonalcoholic fatty liver disease: A comparison of supersonic shear imaging, FibroScan, and ARFI with liver biopsy. *Hepatology* 2016; **63**: 1817-1827 [PMID: 26659452 DOI: 10.1002/hep.28394]
- 22 **Ferraioli G**, Wong VW, Castera L, Berzigotti A, Sporea I, Dietrich CF, Choi BI, Wilson SR, Kudo M, Barr RG. Liver Ultrasound Elastography: An Update to the World Federation for Ultrasound in Medicine and Biology Guidelines and Recommendations. *Ultrasound Med Biol* 2018; **44**: 2419-2440 [PMID: 30209008 DOI: 10.1016/j.ultrasmedbio.2018.07.008]
- 23 **Ronot M**, Di Renzo S, Gregoli B, Duran R, Castera L, Van Beers BE, Vilgrain V. Characterization of fortuitously discovered focal liver lesions: additional information provided by shearwave elastography. *Eur Radiol* 2015; **25**: 346-358 [PMID: 25231131 DOI: 10.1007/s00330-014-3370-z]
- 24 **Guibal A**, Boullaran C, Bruce M, Vallin M, Pilleul F, Walter T, Scoazec JY, Boublay N, Dumortier J, Lefort T. Evaluation of shearwave elastography for the characterisation of focal liver lesions on ultrasound. *Eur Radiol* 2013; **23**: 1138-1149 [PMID: 23160662 DOI: 10.1007/s00330-012-2692-y]
- 25 **Cui YY**, He NA, Ye XJ, Hu L, Xie L, Zhong W, Zhang CX. Evaluation of Tissue Stiffness Around Lesions by Sound Touch Shear Wave Elastography in Breast Malignancy Diagnosis. *Ultrasound Med Biol* 2022; **48**: 1672-1680 [PMID: 35672199 DOI: 10.1016/j.ultrasmedbio.2022.04.219]
- 26 **Ohno E**, Kawashima H, Ishikawa T, Mizutani Y, Iida T, Nishio R, Uetsuki K, Yashika J, Yamada K, Yoshikawa M, Gibo N, Aoki T, Kataoka K, Mori H, Takada Y, Aoi H, Takahashi H, Yamamura T, Furukawa K, Nakamura M, Shimoyama Y, Hirooka Y, Fujishiro M. The role of EUS elastography-guided fine needle biopsy in the histological diagnosis of solid pancreatic lesions: a prospective exploratory study. *Sci Rep* 2022; **12**: 16603 [PMID: 36198904 DOI: 10.1038/s41598-022-21178-4]
- 27 **Mendy ME**, Welzel T, Lesi OA, Hainaut P, Hall AJ, Kuniholm MH, McConkey S, Goedert JJ, Kaye S, Rowland-Jones S, Whittle H, Kirk GD. Hepatitis B viral load and risk for liver cirrhosis and hepatocellular carcinoma in The Gambia, West Africa. *J Viral Hepat* 2010; **17**: 115-122 [PMID: 19874478 DOI: 10.1111/j.1365-2893.2009.01168.x]
- 28 **Pereira Tde A**, Witek RP, Syn WK, Choi SS, Bradrick S, Karaca GF, Agboola KM, Jung Y, Omenetti A, Moylan CA, Yang L, Fernandez-Zapico ME, Jhaveri R, Shah VH, Pereira FE, Diehl AM. Viral factors induce Hedgehog pathway activation in humans with viral hepatitis, cirrhosis, and hepatocellular carcinoma. *Lab Invest* 2010; **90**: 1690-1703 [PMID: 20697376 DOI: 10.1038/labinvest.2010.147]
- 29 **Beste LA**, Leipertz SL, Green PK, Dominitz JA, Ross D, Ioannou GN. Trends in burden of cirrhosis and hepatocellular carcinoma by underlying liver disease in US veterans, 2001-2013. *Gastroenterology* 2015; **149**: 1471-1482.e5; quiz e17 [PMID: 26255044 DOI: 10.1053/j.gastro.2015.07.056]
- 30 **Kanwal F**, Kramer JR, Mapakshi S, Natarajan Y, Chayanupatkul M, Richardson PA, Li L, Desiderio R, Thrift AP, Asch SM, Chu J, El-Serag HB. Risk of Hepatocellular Cancer in Patients With Non-Alcoholic Fatty Liver Disease. *Gastroenterology* 2018; **155**: 1828-1837.e2 [PMID: 30144434 DOI: 10.1053/j.gastro.2018.08.024]
- 31 **Chon YE**, Jung ES, Park JY, Kim DY, Ahn SH, Han KH, Chon CY, Jung KS, Kim SU. The accuracy of noninvasive methods in predicting the development of hepatocellular carcinoma and hepatic decompensation in patients with chronic hepatitis B. *J Clin Gastroenterol* 2012; **46**: 518-525 [PMID: 22688146 DOI: 10.1097/MCG.0b013e31825079f1]
- 32 **Ji F**, Liang Y, Fu SJ, Guo ZY, Shu M, Shen SL, Li SQ, Peng BG, Liang LJ, Hua YP. A novel and accurate predictor of survival for patients with hepatocellular carcinoma after surgical resection: the neutrophil to lymphocyte ratio (NLR) combined with the aspartate aminotransferase/platelet count ratio index (APRI). *BMC Cancer* 2016; **16**: 137 [PMID: 26907597 DOI: 10.1186/s12885-016-2189-1]
- 33 **Kim JH**, Kim YD, Lee M, Jun BG, Kim TS, Suk KT, Kang SH, Kim MY, Cheon GJ, Kim DJ, Baik SK, Choi DH. Modified PAGE-B score predicts the risk of hepatocellular carcinoma in Asians with chronic hepatitis B on antiviral therapy. *J Hepatol* 2018; **69**: 1066-1073 [PMID: 30075230 DOI: 10.1016/j.jhep.2018.07.018]
- 34 **Shindoh J**, Andreou A, Aloia TA, Zimmitti G, Lauwers GY, Laurent A, Nagorney DM, Belghiti J, Cherqui D, Poon RT, Kokudo N, Vauthey JN. Microvascular invasion does not predict long-term survival in hepatocellular carcinoma up to 2 cm: reappraisal of the staging system for solitary tumors. *Ann Surg Oncol* 2013; **20**: 1223-1229 [PMID: 23179993 DOI: 10.1245/s10434-012-2739-y]
- 35 **Hu HT**, Wang Z, Huang XW, Chen SL, Zheng X, Ruan SM, Xie XY, Lu MD, Yu J, Tian J, Liang P, Wang W, Kuang M. Ultrasound-based radiomics score: a potential biomarker for the prediction of microvascular invasion in hepatocellular carcinoma. *Eur Radiol* 2019; **29**: 2890-2901 [PMID: 30421015 DOI: 10.1007/s00330-018-5797-0]
- 36 **Feng ST**, Jia Y, Liao B, Huang B, Zhou Q, Li X, Wei K, Chen L, Li B, Wang W, Chen S, He X, Wang H, Peng S, Chen ZB, Tang M, Chen Z,

- Hou Y, Peng Z, Kuang M. Preoperative prediction of microvascular invasion in hepatocellular cancer: a radiomics model using Gd-EOB-DTPA-enhanced MRI. *Eur Radiol* 2019; **29**: 4648-4659 [PMID: 30689032 DOI: 10.1007/s00330-018-5935-8]
- 37 **Ma X**, Wei J, Gu D, Zhu Y, Feng B, Liang M, Wang S, Zhao X, Tian J. Preoperative radiomics nomogram for microvascular invasion prediction in hepatocellular carcinoma using contrast-enhanced CT. *Eur Radiol* 2019; **29**: 3595-3605 [PMID: 30770969 DOI: 10.1007/s00330-018-5985-y]
- 38 **Lee JS**, Lee HW, Lim TS, Shin HJ, Lee HW, Kim SU, Park JY, Kim DY, Ahn SH, Kim BK. Novel Liver Stiffness-Based Nomogram for Predicting Hepatocellular Carcinoma Risk in Patients with Chronic Hepatitis B Virus Infection Initiating Antiviral Therapy. *Cancers (Basel)* 2021; **13** [PMID: 34885000 DOI: 10.3390/cancers13235892]
- 39 **Kumada T**, Toyoda H, Yasuda S, Ogawa S, Gotoh T, Tada T, Ito T, Sumida Y, Tanaka J. Combined ultrasound and magnetic resonance elastography predict hepatocellular carcinoma after hepatitis C virus eradication. *Hepatol Res* 2022; **52**: 957-967 [PMID: 35841314 DOI: 10.1111/hepr.13814]



Published by **Baishideng Publishing Group Inc**
7041 Koll Center Parkway, Suite 160, Pleasanton, CA 94566, USA
Telephone: +1-925-3991568
E-mail: office@baishideng.com
Help Desk: <https://www.f6publishing.com/helpdesk>
<https://www.wjgnet.com>

